Soft Matter

Accepted Manuscript

This is an *Accepted Manuscript*, which has been through the Royal Society of Chemistry peer review process and has been accepted for publication.

Accepted Manuscripts are published online shortly after acceptance, before technical editing, formatting and proof reading. Using this free service, authors can make their results available to the community, in citable form, before we publish the edited article. We will replace this *Accepted Manuscript* with the edited and formatted *Advance Article* as soon as it is available.

You can find more information about *Accepted Manuscripts* in the Information for Authors.

Please note that technical editing may introduce minor changes to the text and/or graphics, which may alter content. The journal's standard Terms & Conditions and the Ethical guidelines still apply. In no event shall the Royal Society of Chemistry be held responsible for any errors or omissions in this *Accepted Manuscript* or any consequences arising from the use of any information it contains.

ROYAL SOCIETY OF CHEMISTRY

www.rsc.org/softmatter

Colloidal Structures of Asymmetric Dimers via Orientation-dependent Interactions

Fuduo Ma,[1] Sijia Wang,[1] Hui Zhao,[2] David T. Wu,[3] and Ning Wu[1,*]

[1]Department of Chemical and Biological Engineering, Colorado School of Mines, Golden, Colorado 80401

[2]Department of Mechanical Engineering, University of Nevada, Las Vegas, Nevada 89154

[3]Department of Chemistry and Geochemistry, Colorado School of Mines, Golden, Colorado 80401

Soft Matter Accepted Manuscript

Abstract

We apply an AC electric field to induce anisotropic interactions among asymmetric colloidal dimers. These anisotropic interactions, being shape-specific and orientation-dependent, can create complex and unique structures that are not possible for spherical particles or symmetric dimers. More specifically, we show a series of novel structures that closely resemble one- and two-dimensional antiferromagnetic lattices, including small clusters, linear chains, squares, and frustrated triangular arrays. All of them are uniquely formed by alternating association between dimers with opposite orientations. Our theoretical model attributes those patterns to an exquisite balance between electrostatic (primarily dipolar) and electrohydrodynamic interactions. Although similarly oriented dimers are strongly repulsive, the oppositely oriented dimers possess a concave shoulder in the pair interaction, which favors clustering to minimize the number of overlaps between neighboring particles. By combining the anisotropy in both particle geometry and field-induced interaction, our work suggests a new way to tailor colloidal interactions on anisotropic particles, which is important for both scientific understanding and practical applications.

Introduction

Studies on colloidal particles have shed light on the physics of soft materials, including crystal nucleation and growth, phase behavior, and glass formation.[1-3] In particular, particles with anisotropy in geometry, surface functionality, or chemical composition can potentially mimic natural interactions between molecules, which are often shape-specific and orientation-dependent. Pioneering work on their assembly has shown intriguingly non-close packed structures and well-controlled colloidal molecules[4-10] that are not imaginable for isotropic particles. However, most assembly work has relied on intrinsic colloidal interactions, which are often weak, of short range, and slow in assembly kinetics. The range of morphologies obtained to date is far from the diversity of structures desired for either fundamental understanding or technological application. Compared with self-assembly, directed-assembly using external fields affords tuning both the strength and effective range of colloidal interactions over several orders of magnitude.[11-13] Moreover, applied fields, such as an electric field, can induce anisotropic interactions even on intrinsically isotropic spheres.[14] Therefore, a powerful way to access previously formidable phase space is to combine external fields with particles that possess anisotropic properties.

Arguably, the simplest form of an anisotropic particle beyond a sphere is a colloidal dimer where two lobes are grown together. Indeed, they have been assembled, under external fields, into a variety of exotic two- and three-dimensional structures.[6, 10, 15-18] Most of the work, however, has employed dimer particles with symmetric lobe sizes. The full degree of geometric anisotropy on colloidal dimer has not been exploited. Since nowadays the bulk synthetic methods have been advanced enough that various types of

Soft Matter Accepted Manuscript

anisotropic properties can be created on dimers in a precise fashion,[19-24] it becomes possible to assemble dimers into more complex and innovative patterns. In order to achieve this goal, however, a deep understanding of the combined impacts of particle asymmetry and field-induced interactions is necessary.

In this paper, we investigate the directed-assembly of asymmetric colloidal dimers under the influence of AC electric fields. By combining the anisotropy in both particle geometry and field-induced electrostatic/hydrodynamic interactions, we show a variety of novel structures that closely resemble one- and two-dimensional antiferromagnetic lattices. To understand the underlying physics of the structural formation, we develop a theoretical model based on the energy of collective interactions. Our model reveals that the overall pair interactions between asymmetric dimers depend sensitively on their relative orientations. Moreover, the potential between oppositely oriented dimers consists of a concave shoulder with two different length scales, which well explains the unique structures that we observe in experiments.

Methods and Materials

Dimer synthesis The synthesis of asymmetric dimers is performed in a two-step seeded emulsion polymerization.[17, 22, 24] In brief, spherical polystyrene particles (the seeds) are first synthesized by the dispersion polymerization in a mixture of methanol and water. The spherical particles are then cross-linked by divinylbenzene (DVB) and 3-(trimethoxysilyl) propylacrylate (TMSPA). The crosslinked polystyrene spheres (CPS) are swollen by an aqueous emulsion of styrene, sodium styrene sulfonate, and initiator (2,2′-Azobis(2.4-dimethyl valeronitrile)) stabilized by both polyvinyl alcohol and sodium dodecyl sulfate. After mixing the emulsion with CPS solutions, a second liquid

Soft Matter Accepted Manuscript

lobe appears on the original CPS particle. Further polymerization solidifies the shape of colloidal dimers. The amount of styrene in the swelling stage is varied to generate asymmetric dimers with different aspect ratios.

Characterization Both the morphologies and sizes of asymmetric dimers are examined using SEM (JEOL JSM-7000F). Positively charged fluorescent dyes are coated on the dimers. Almost equal fluorescence intensities indicate balanced surface charges on both lobes. The electrophoretic mobilities of particles in deionized water is measured via a Zetasizer (Brookhaven 90Plus PALS). Zeta potentials are then calculated from mobility measurements according to the methods suggested in literature.[25]

Electric field assembly A thin film of asymmetric dimer suspension is placed between two parallel pieces of ITO glasses. An insulating polymer film is used as the spacer. The spacer's thickness is ~ 100 μm. ITO glasses are purchased from Sigma-Aldrich with surface resistivity of 15-25 Ω/sq. ITO glasses are ultrasonically cleaned in acetone and isopropanol for 20 minutes, followed by oxygen plasma cleaning for 1 minutes. The AC electric field is applied between two ITO glasses by a function generator (RTGOL DG 1022). Real time observations are performed on an inverted microscope (Olympus IX 71) and recorded with a CCD camera (Retiga 2000R).

Results and Discussion

Structures formed by oppositely oriented dimers

The inset in Fig. 1a shows a representative SEM image of the asymmetric polystyrene dimers used in our experiments (R_1 ~1.27μm and R_2 ~0.89μm). They are synthesized by seeded emulsion polymerization[22] with polydispsersity less than 1.1.The dimers are then suspended in deionized water before sandwiching between two indium

Soft Matter Accepted Manuscript

tin oxide (ITO) glass slides. An insulating polyester film ($2H \sim 100\mu m$) is used as a spacer to separate these two electrodes. Although $H \square R_i$, we purposely choose the particle concentration so that only a monolayer can be formed on the substrate for the convenience of optical characterization. We calculate the particle density η based on the volume fraction of standing dimers within the monolayer over an area of at least 200×150 μm^2. An external AC bias $V_p e^{-j\omega t}$ is applied perpendicularly across both top and bottom electrodes, where V_p is the peak voltage and ω is the frequency. With high enough frequency and voltage (ω>2 kHz and V_p>4 V), the electrostatic torque is strong enough that all dimers are aligned with the external field, i.e., they stand on the bottom substrate. Because the dimers are asymmetric, the large lobe can either face toward or away from the bottom substrate, adopting two standing orientations ("up" and "down") with approximately equal probabilities (Fig. 1b).

At $\eta \sim 12\%$, we observe a variety of clusters of associating dimers as shown in Fig. 1a. Close examination reveals that all neighboring dimers within those clusters adopt alternating orientations (Fig. 1b). This is exemplified by the high population of dimer doublets, where an "up" dimer is closely paired with a "down" dimer. In contrast, standing dimers with the same orientations (either "up" or "down") repel each other and form well-separated arrays, as shown in the top right of Fig. 1b. The formation of dimer doublets and other clusters clearly indicates that the pair interaction between standing dimers is anisotropic: it strongly depends on the relative orientations of the neighboring dimers.

To further understand the orientation-dependent interactions between asymmetric dimers, we study their assembly at various particles densities. Representative snapshots

Soft Matter Accepted Manuscript

with high magnifications are shown in Fig. 2. At very low density ($\eta \sim 1\%$), the standing dimers are in the "gas" phase. When η is increased to 6%, they are well-separated with an average spacing of $\sim 2.6 D_1$ (where D_1 is the diameter of the large lobe), indicating that both "up" and "down" dimers experience long-range repulsions. At $\eta \sim 13\%$, we start to observe the association between "up" and "down" dimers when they are close enough. Those with the same orientations, however, still remain separated. This specific association between oppositely oriented dimers becomes further evident at higher particle densities, where large areas of linear chains ($\eta \sim 15\%$) and square crystals ($\eta \sim 30\%$) are observed. With the unique arrangement of alternating "up" and "down" dimers, these structures closely resemble one- and two-dimensional antiferromagnetic lattices,[26] where the "up" and "down" spins are represented by the corresponding two standing orientations of asymmetric dimers.

The structures formed between "up" and "down" dimers can be tuned by both field strength and frequency. When the applied voltage is decreased from 10 V to 5 V, we observe qualitatively similar phases at different particle densities (SI Fig. S1a). However, dimer interactions weaken. For example, the mass-averaged length of alternating chains decreases from 4.5 to 2.3. Much longer chains can only be observed at higher field strengths (SI Fig. S1b). The square crystals are also less ordered at 5 V, where the orientational bond order parameter ψ_4 decreases from 0.94 to 0.75. Frequency can also affect the structure. As shown in Fig. 3a-b, the square lattices can transform into triangular arrays at higher frequencies. Although the distance between "up" and "down" dimers barely changes with increasing frequency, the "up-up" and "down-down" separations decrease significantly (Fig. 3d). The triangular lattice, however, is a frustrated

Soft Matter Accepted Manuscript

structure for the antiferromagnetic Ising system because one of the three neighboring dimers cannot be simultaneously antiparallel to the other two. The antiferromagnetic Ising model on a triangular lattice has a highly degenerate ground states with each ground state configuration having one frustrated bond per plaquette.[26] The condition still leaves nearly all ground state configurations as disordered. However, the triangular lattice shown in Fig. 3b is clearly not random. It is composed of alternating rows of "up" and "down" dimers that form zigzag stripes with random sidewise stacks (Fig. 3c). If we consider a neighboring dimer pair with the same orientation as one frustrated bond, the average number of frustrated bonds per particle is ~2.2 for Fig. 3c. In comparison, the high-temperature limit of a purely random triangular lattice has an average number of 3. It is interesting to note that our zigzag stripes are analogous to those seen in the buckled monolayers of spherical colloids under geometric confinement.[27] Although our system is not geometrically confined, the "up-down" arrangement of standing dimers forms an effectively buckled monolayer for both large and small lobes. It has been suggested that the out-of-plane buckling can induce an in-plane lattice distortions that favor zigzag stripes and partially relieve the ground-state degeneracy of frustrated Ising models.[28]

Our experiments raise several intriguing questions, among which the most important one is: what is the origin of the effective interaction that leads to the rich patterns formed only between "up" and "down" asymmetric dimers? In fact, these pattern are uniquely observed for asymmetric dimers. For example, when we use symmetric dimers under the same experimental conditions, we do not observe any aggregation (Fig. S2a) until $\omega > 9000$ Hz where triangular lattices of standing dimers are found. For spherical particles, we observe the formation of colloidal trimers in which a central

Soft Matter Accepted Manuscript

sphere sits on top of two bottom spheres (Fig. S2b), indicating a strong out-of-plane dipolar attraction between particles. Both results of symmetric dimers and spheres are consistent with our previous publications[14, 17] but are very different from what we have observed here. Therefore, it is reasonable to assume that the geometric anisotropy of dimers, potentially possessing orientation-dependent interactions, leads to the characteristic Ising-like lattices.

Before building a theoretical model to understand the pattern formation mechanism, we first briefly review the important forces involved in the electric-field assembly of colloids in general. They often include the screened Coulomb, dipolar, and electrohydrodynamic (EHD) interactions.[12] The screened Coulomb interaction is expected to be independent of particle orientations. Both "up" and "down" dimers should feel similar repulsive forces once their separations are comparable to the Debye length κ^{-1} (~150 nm here). The dipolar interaction between particles can be attractive or repulsive, depending on the angle θ between the center-to-center line that connects two particles and the applied field direction.[12] Therefore, it is orientation-dependent. The vertical offsets between neighboring large and small lobes in the "up-down" configuration could potentially generate an attractive dipolar interaction between oppositely oriented dimers. The third important force is the EHD interaction. This force arises from the EHD flow of ions and solvent close to the conducting substrate. The applied electric field induces a large amount of mobile charges within the Debye layer at low frequencies. The tangential component of the electric field generated from the polarized particles acts on the induced charges and creates an EHD flow along the substrate. This EHD flow with sufficient strength could cause aggregation or segregation

Soft Matter Accepted Manuscript

of particles.[29, 30] Although the EHD flow originates from the diffusive layer near the electrode, the polarized "up" and "down" dimers could, in principle, generate tangential electric fields with different strengths and make the EHD interaction depend on dimer's orientation too.

Theoretical Model and Monte Carlo Simulation

Here, we first present a theoretical model to study the potentially anisotropic nature of the dipolar and EHD interactions between asymmetric dimers. With additional incorporation of the (isotropic) screened Coulomb interaction, we aim to model the effective potential between a pair of dimers with different orientations, which will be tested in two-dimensional Monte Carlo simulations. As shown in Fig. 4a, we approximate individual lobes on dimer particles as spheres. The dimers are suspended in a fluid with dielectric constant ε, Debye length κ^{-1}, viscosity μ, and are subject to an applied field $\mathbf{E}_0(\mathbf{r}) = -\nabla\psi_0(\mathbf{r})$, where $\psi_0(\mathbf{r})$ is the electrostatic potential. Each sphere i at the position $\mathbf{r}_i$, has fixed properties of radius R_i and effective charge q_i. The polarizability of the sphere i is given by $\alpha_i = 4\pi\varepsilon_0\varepsilon R_i^3 K_i$, where the polarization coefficient K_i depends on the radius, frequency, Debye length, and zeta potential ζ_i.[31-33] At low frequencies (i.e., in the current experimental regime), K_i can be calculated analytically using the modified Dukhin-Shilov theory[33] or numerically by solving the standard electrokinetic model.[31] Two spheres approximating lobes on the same dimer are subject to the geometric constraint $\left|\mathbf{r}_i - \mathbf{r}_j\right| = R_i + R_j$. The interaction between dimers and the conducting substrate is accounted for by adding image charges and dipoles (grey spheres in Fig. 4a) underneath the electrode (and included in the sums over charges below). The dipole on

Soft Matter Accepted Manuscript

sphere i, $\mathbf{p}_i$, is induced by the electric fields that are applied externally, arisen from neighboring charges, and generated by neighboring dipoles,

$$\mathbf{p}_i = \alpha_i \left\{ \mathbf{E}_0(\mathbf{r}_i) + \sum_{j \neq i} \left[\mathbf{E}_{Y,j}(\mathbf{r}_i) + \mathbf{E}_{ind,j}(\mathbf{r}_i) \right] \right\} \quad (1)$$

where $\mathbf{E}_{Y,j}(\mathbf{r}) = -\nabla \psi_{Y,j}(\mathbf{r} - \mathbf{r}_j)$ is the field arising from the Yukawa-type [34] screened charge q_j corresponding to the Yukawa potential $\psi_{Y,j}(r) = q_j \exp(-\kappa r)/r$ and $\mathbf{E}_{ind,j}(\mathbf{r}) = \mathbf{T}(\mathbf{r} - \mathbf{r}_j) \cdot \mathbf{p}_j$ is the field generated by the induced dipole j. Here the kernel for the dipole field is given by $\mathbf{T}(\mathbf{r}) = (3\mathbf{rr} - \mathbf{I})/4\pi\varepsilon\varepsilon_0 |\mathbf{r}|^3$. Since induced dipoles interact mutually and respond to local electric fields, we need to solve for them self-consistently. For a given spatial configuration of particles, the induced dipoles can be obtained by solving a system of linear equations for $\mathbf{p}_i$

$$\mathbf{p}_i = \sum_j \mathbf{A}_{ij} \cdot \left[\mathbf{E}_0(\mathbf{r}_j) + \sum_{k \neq j} \mathbf{E}_{Y,k}(\mathbf{r}_j) \right] \quad (2)$$

where $\mathbf{A}_{ij} = \left[\alpha_i^{-1} \delta_{ij} - \mathbf{T}(\mathbf{r}_i - \mathbf{r}_j)(1 - \delta_{ij}) \right]^{-1}$ is a collective polarizability tensor for the entire system of colloidal spheres.

Once $\mathbf{p}_i$ is obtained, the electrostatic energy U_e for the system of dimers can then be written

$$U_e(\{\mathbf{r}_i; \mathbf{p}_i\}) = \frac{1}{2} \left[U_{SC}(\{\mathbf{r}_i; \mathbf{p}_i\}) + U_d(\{\mathbf{r}_i; \mathbf{p}_i\}) \right] \quad (3)$$

where the energy due to screened charges U_{SC} includes the charge-applied field, charge-charge, and charge-dipole interactions.

Soft Matter Accepted Manuscript

$$U_{SC}\left(\{\mathbf{r}_i;\mathbf{p}_i\}\right)=\sum_i q_i\psi_0\left(\mathbf{r}_i\right)+\sum_i\sum_{j>i} q_i\psi_{Y,j}\left(\mathbf{r}_i-\mathbf{r}_j\right)-\frac{1}{2}\sum_i \mathbf{p}_i\cdot\sum_{j\neq i} E_{Y,j}\left(\mathbf{r}_i\right) \qquad (4)$$

The energy U_d includes dipole-applied field, dipole-dipole interactions, and a harmonic self-energy that corresponds to the assumption of linear polarizability, respectively.

$$U_d\left(\{\mathbf{r}_i;\mathbf{p}_i\}\right)=-\sum_i \mathbf{p}_i\cdot\mathbf{E}_0-\frac{1}{2}\sum_{i\neq j}\mathbf{p}_i\cdot\mathbf{T}\left(\mathbf{r}_i-\mathbf{r}_j\right)\mathbf{p}_j+\frac{1}{2}\sum_i \mathbf{p}_i\cdot\alpha_i^{-1}\cdot\mathbf{p}_i \qquad (5)$$

The factor 1/2 in Eq. (3) arises from the fact that the sums taken above for the total system includes contributions from both real particles and their (charge and dipole) images.

An example of the self-consistent calculation of the induced dipoles and the corresponding local electric fields is shown in SI Fig. S3. Parameters used in the calculations correspond to typical experiment conditions: $R_1=1.27\,\mu\text{m}$, $R_2=0.89\,\mu\text{m}$, $\zeta_1=\zeta_2=-60\,\text{mV}$, $\varepsilon=78$, $V_p=8\text{ V}$, $2H=100\,\mu\text{m}$, $\omega=$ 6.5k Hz, and $\kappa^{-1}\sim 150\,\text{nm}$. It can be seen that all dipoles are slightly tilted rather than perfectly aligned with the applied field due to the influence of neighboring dipoles. The calculated dipoles and local electric fields also allow us to compute the electrostatic interaction between two standing dimers with predefined orientations and separations. Fig. 4a shows that the electrostatic interaction between "down-down" dimers is strongly repulsive for all separations. It is dominated by dipolar repulsion. The screened Coulomb repulsion is strong only at very short separations (within hundreds nm). Fig. 4a also shows that the interaction is primarily controlled by the dipolar repulsion between large lobes U_d^{13}. Although U_d^{14} and U_d^{17} can be negative when their center-to-center lines become more aligned with the applied field at smaller separations, they are relatively weak. This is expected since the

Soft Matter Accepted Manuscript

dipolar interaction between two lobes is proportional to the volumes of particle i and j. Moreover, the polarization coefficient K_i depends on κR_i sensitively,[33] which further highlights the importance of the dipolar interaction between large lobes. Similarly, the interaction between "up-up" dimers is also strongly repulsive (SI Fig. S4). The "up-down" interaction, however, is in stark contrast (Fig. 4b). At intermediate separations, both U_d^{13} and U_d^{17} are strongly attractive because of the vertical offset between two large lobes. They significantly soften the electrostatic potential U_e and lead to the appearance of a point of inflection. Such a softened dipolar interaction has a profound impact on the overall interaction between oppositely-oriented dimers, as we will show later. Again, at even smaller separations, the screened double layer interaction is dominant and leads to the hard core repulsion.

Next, we examine the EHD interaction between asymmetric dimers. We extend the established theory for spherical particles[29, 35] and derive the EHD interaction between "up" or "down" dimers. The derivation details are shown in the supplementary information, and we summarize our key results here. The applied voltage $V_p e^{-j\omega t}$ will induce diffusive charges near the electrode, which is frequency-dependent

$$q = -\varepsilon\varepsilon_0 \frac{V_p}{2H} e^{-j\omega t} \frac{\kappa H\left(1+j\beta\right)}{1+\beta^2} \tag{6}$$

where $j=\sqrt{-1}$, $\beta = \omega H / \kappa D$, and D is the diffusivity of the ions. As expected, the induced charges decrease with increasing frequencies. A tangential electric field, arising from the tangential component of the field generated by the induced dipole of a standing dimer, acts on the induced charges and initiates the EHD flow of solvent. For an "up"

Soft Matter Accepted Manuscript

dimer, this tangential field is the sum of two dipolar fields from both large and small lobes

$$\begin{aligned} E_{t,\mathrm{up}} &\sim E_{dipole,up}\cdot\hat{x}\sim\left(E_{dipole,1}+E_{dipole,2}\right)\cdot\hat{x} \\ &\sim -\frac{V_p}{2H}e^{-j\omega t}\frac{\beta^2-j\beta}{1+\beta^2}\left[\left(K_1'+jK_1''\right)f_1(r)+\left(K_2'+jK_2''\right)g_2(r)\right] \end{aligned} \tag{7}$$

where $\hat{x}$ is a unit vector in the x direction along the substrate (SI Fig. S7), $K_i = K_i' + jK_i''$ is the complex polarization coefficient[32, 36] of lobe i. Similarly, the tangential electric field from a "down" dimer is

$$E_{t,\mathrm{down}} \sim -\frac{V_p}{2H}e^{-j\omega t}\frac{\beta^2-j\beta}{1+\beta^2}\left[\left(K_2'+jK_2''\right)f_2(r)+\left(K_1'+jK_1''\right)g_1(r)\right] \tag{8}$$

In both equations, $f_i(r)$ and $g_i(r)$, given in SI Eq. (S10) and Eq. (S11), dictate the r-dependence of the tangential field. The EHD velocities for both "up" and "down" dimers are proportional to the product of the induced charges and the tangential field

$$u_{EHD}^{up} \sim \frac{\langle q\cdot E_t\rangle}{\mu\kappa} = \frac{\mathrm{Re}\left(q\cdot E_t^*\right)}{2\mu\kappa} = \frac{C}{2\mu}\left[\mathrm{K}_1''f_1(r)+K_2''g_2(r)\right] \tag{9}$$

and

$$u_{EHD}^{down} \sim \frac{\mathrm{C}}{2\mu}\left[\mathrm{K}_2''f_2(r)+K_1''g_1(r)\right] \tag{10}$$

where $C=\varepsilon\varepsilon_0\left(\frac{V_p}{2H}\right)^2\frac{\beta^2}{1+\beta^2}\frac{\kappa D}{\omega}$. After calculating the EHD velocity $u_{EHD}(r)$, we can estimate the drag force on a dimer. Since there is no analytical expression for a colloidal dimer, we approximate it with an oblate spheroid. The lengths of its semi-major and semi-minor axes are a and b, respectively. At low Reynolds number, the drag force on an oblate spheroid due to a transverse flow is:[37] $F(r)=6\pi\mu u_{EHD}(r)af(e)$, where e is the

Soft Matter Accepted Manuscript

eccentricity, i.e., $e=\sqrt{1-\left(b/\mathrm{a}\right)^2}$. For a sphere, $e=0$ and $f\left(e\right)=1$. The effective EHD interaction potential between two particles is obtained by integrating this force, i.e., $\phi_{EHD}\left(r\right)=\int_r^\infty F\left(r'\right)dr'$.[35] For "up" dimers, it can be expressed

$$\phi_{EHD}^{up}(r)\sim 3\pi af\left(e\right)C\left\{\frac{\mathrm{K_1"}R_1}{\left[1+\left(r/R_1\right)^2\right]^{3/2}}+\frac{K_2"R_2\left(2R_1/R_2+1\right)}{\left[\left(2R_1/R_2+1\right)^2+\left(r/R_2\right)^2\right]^{3/2}}\right\} \qquad (11)$$

The EHD interaction between "down" dimers is

$$\phi_{EHD}^{down}(r)\sim 3\pi af\left(e\right)C\left\{\frac{\mathrm{K_2"}R_2}{\left[1+\left(r/R_2\right)^2\right]^{3/2}}+\frac{K_1"\mathrm{R}_1\left(2R_2/R_1+1\right)}{\left[\left(2R_2/R_1+1\right)^2+\left(r/R_1\right)^2\right]^{3/2}}\right\} \qquad (12)$$

Fig. 5a shows the EHD interaction between a pair of "up" dimers. The individual contributions of each lobe (the first and second terms in RHS of Eq. 11) are also included. Clearly, the bottom large lobe has a major influence due to both a stronger dipolar field and a closer distance to the substrate. For the EHD interaction between a pair of "down" dimers (Fig. 5b), although the large lobe is further away from the substrate, its dipolar field is stronger. Therefore, both lobes contribute almost equally. Interestingly, the EHD interactions (red curves) in Fig. 5a and 5b are very similar except at very short separations. Since we assume that the induced charges on the electrode do not depend on the orientation of the dimer, this result indicates that the tangential field generated by an "up" or "down" dipole does not differ much. Unlike the dipolar interaction, our result shows that the EHD interaction does not sensitively depend on the orientation of dimers.

With both electrostatic and EHD interactions, we can add them together to calculate the overall interaction between a pair of dimers with different orientations.

Soft Matter Accepted Manuscript

Shown in Fig. 6, the "up-up" and "down-down" interactions are purely repulsive, which indicates that the EHD attraction is too weak to overcome the dipolar repulsion for both configurations. The "up-down" configuration, however, is very different. Because of the much softened dipolar interaction shown in Fig. 4b, a concave shoulder develops when the EHD attraction becomes strong at smaller separations, and can lead to a potential minimum of varying depth just inside the shoulder. We note that this potential closely resembles the so-called core-softened potential, which can arise in colloids such as magnetic spheres in a confined cell[38] and in molecules such as water.[39] Compared with the "up-up" and "down-down" interactions, this concavity induces an attractive force that clearly favors the alternating association between "up" and "down" dimers into square arrays at high particle densities. Moreover, this "up-down" potential consists of two length scales: the hard-core diameter and the concave shoulder, which have a profound influence on the patterns formed at intermediate particle densities too.[40] Instead of a uniform particle distribution where all shoulders are partially overlapped, dimers are assembled into alternating clusters and linear chains with characteristically large inter-chain separations (SI Fig. S5). According to computation,[40] this configuration allows the minimization of overlaps between shoulders and corresponds to the lowest possible energy state.

To validate the above-derived pair potential between dimers with different orientations, we further perform Monte Carlo simulations. Since dimers form a monolayer on the conducting substrate in experiments, in our simulations they are allowed to move freely along the $x-y$ plane but not in the direction perpendicular to the substrate. An equal mixture of "up" and "down" dimers ($N_{tot}=256$) are placed in a

Soft Matter Accepted Manuscript

square simulation cell of area $A = L^2$. Therefore, the simulation is effectively two dimensional (*NAT*). The equilibrium structures (after 50000 cycles) at different particle densities η are shown in Fig. 7, which clearly illustrates the preferential association between "up" and "down" dimers. At low densities, they mostly form into doublets. As density increases, longer chains with alternating arrangement of "up" and "down" dimers can be seen. More importantly, the chains are well-separated from each other with a characteristic spacing. At high densities, square lattices emerge. Clearly, the simulation results match faithfully with our experimental images in Fig. 2, which validate the orientation-dependent interactions between asymmetric dimers.

Discussion

The concavity of the shoulder depends on several parameters, which can significantly influence the orientation-dependent dipolar interaction. For example, the particles are not necessarily separated from the electrode with the same distances.[30, 35] As shown in Fig. 8a, when one of the dimers is lifted slightly above the substrate even by a few hundred nanometers, the stronger dipolar attraction between large lobes can further soften the electrostatic interaction and eventually lead to a short-range attraction. In fact, for larger dimers ($R_1 \sim 2$ μm) with stronger dipolar interactions we observe significant overlap between "up" and "down" dimers, which indicates a vertical displacement between them (the inset of Fig. 8a). When a dimer is asymmetric not only in geometry but also in interfacial property such as the zeta potential, the polarization coefficient K_i between two lobes could also be very different.[32, 41] For example, with a fixed K_1 (-0.21) and increasing K_2 from negative to positive, the dipolar interactions between "up" and "down" dimers becomes strongly attractive (Fig. 8b). Similar to the up and down spins in

Soft Matter Accepted Manuscript

the Ising model, now the small and large lobes with oppositely-oriented dipoles will attract each other. Considering that the "up-up" and "down-down" interactions could still be highly repulsive in this scenario, we expect to see the formation of square Ising lattices due to this "up-down" attraction. In fact, when $K_2 = 0$, the dipolar interactions arising from small lobes disappear. Our system would effectively reduce to the buckled magnetic spheres in a quasi-planar cell, where both chain-like and square patterns have been observed.[38] Experimentally, a positive polarizability ($K_2 > 0$) can be achieved by synthesizing dimers with asymmetric surface charges, tuning the pH/salt concentration in the solution, or coating one of the lobes with a thin metallic layer.[8] We are currently investigating along these lines.

As our modeling reveals, the Ising-like structures arise from an exquisite competition/balance between anisotropic dipolar interaction and isotropic electrohydrodynamic attraction, where the geometric asymmetry of particles is critical. Such a phenomenon should be universal for asymmetric dimers with intermediate values of R_2 / R_1. As shown in Fig. 9, we consistently observe the alternating aggregation between "up" and "down" dimers for a variety of aspect ratios. Furthermore, it is reasonable to infer that when we change the experimental conditions, we could possibly break the balance between electrostatic and electrohydrodynamic interactions. Correspondingly, we expect to observe different patterns. For example, when we change the suspension medium from water to the less polar solvent dimethyl sulfoxide (DMSO), the concentration of mobile charges is decreased significantly. It is expected that the electrohydrodynamic interaction will be much weaker than the dipolar interaction. Indeed, we observe that the standing dimers are now assembled into zig-zag clusters and linear

Soft Matter Accepted Manuscript

chain where the central dimer is always lifted significantly (Fig. 10a). Clearly, such a configuration is possible because of the strong out-of-plane dipolar attraction between neighboring dimers. In another case, we add more salt (potassium chloride) in water to decrease relative strength of the dipolar and double-layer interactions. At 1 mM salt concentration, we observe the aggregation of all standing dimers into hexagonal arrays with mixtures of "up" and "down" dimers (Fig. 10b). This is not surprising because the electrohydrodynamic flow along the electrode becomes dominant.[29]

Conclusion

In summary, we report a new way to tailor colloidal interactions by combining anisotropy in both particle geometry and external fields. The anisotropic colloidal interactions induces the alternating association between "up" and "down" dimers. Such unique association leads to a rich variety of novel patterns that include small clusters, linear chains, square crystals, and frustrated triangular arrays. Surprisingly, those structures closely resemble one- and two-dimensional antiferromagnetic Ising lattices. The developed theoretical model suggests that this preferential "up-down" association results from an exquisite balance between dipolar and electrohydrodynamic interactions. While the EHD interactions do not differ much for "up" or "down" dimers, the dipolar interaction depends sensitively on the relative orientation between neighboring dimers. Such an orientation-dependent interaction generates unique structures beyond what have been observed before. The colloidal dimers, which can be further tailored with other types of anisotropic properties, could possess much more diversified types of colloidal interactions when combined with external fields. Such a capability is highly desirable for

Soft Matter Accepted Manuscript

both scientific understanding of colloidal assembly and practical fabrication of functional materials.

Acknowledgements

This work is partially supported by the Colorado Center for Revolutionary Solar Photoconversion through a seed grant, by Bay Area Photovoltaic Consortium, and by National Science Foundation (CBET-1336893).

Additional information

Supplementary Information Figures S1-S7.

Reference

1. G. N. Meng, N. Arkus, M. P. Brenner and V. N. Manoharan, *Science*, 2010, **327**, 560-563.
2. P. J. Lu, E. Zaccarelli, F. Ciulla, A. B. Schofield, F. Sciortino and D. A. Weitz, *Nature*, 2008, **453**, 499-503.
3. A. Yethiraj and A. van Blaaderen, *Nature*, 2003, **421**, 513-517.
4. Q. Chen, S. C. Bae and S. Granick, *Nature*, 2011, **469**, 381-384.
5. Y. Wang, Y. Wang, D. R. Breed, V. N. Manoharan, L. Feng, A. D. Hollingsworth, M. Weck and D. J. Pine, *Nature*, 2012, **491**, 51-55.
6. J. D. Forster, J. G. Park, M. Mittal, H. Noh, C. F. Schreck, C. S. O'Hern, H. Cao, E. M. Furst and E. R. Dufresne, *ACS Nano*, 2011, **5**, 6695-6700.
7. A. H. Groschel, A. Walther, T. I. Lobling, F. H. Schacher, H. Schmalz and A. H. E. Muller, *Nature*, 2013, **503**, 247-251.
8. S. Gangwal, A. Pawar, I. Kretzschmar and O. D. Velev, *Soft Matter*, 2010, **6**, 1413-1418.
9. K. Liu, Z. Nie, N. Zhao, W. Li, M. Rubinstein and E. Kumacheva, *Science*, 2010, **329**, 197-200.
10. A. F. Demirors, P. M. Johnson, C. M. van Kats, A. van Blaaderen and A. Imhof, *Langmuir*, 2010, **26**, 14466-14471.
11. M. J. Solomon, *Curr. Opin. Colloid. Interface. Sci.*, 2011, **16**, 158-167.
12. A. Yethiraj, *Soft Matter*, 2007, **3**, 1099-1115.
13. M. Grzelczak, J. Vermant, E. M. Furst and L. M. Liz-Marzan, *ACS Nano*, 2010, **4**, 3591-3605.
14. F. Ma, D. T. Wu and N. Wu, *J. Am. Chem. Soc.*, 2013, **135**, 7839-7842.
15. M. M. Panczyk, J. G. Park, N. J. Wagner and E. M. Furst, *Langmuir*, 2013, **29**, 75-81.
16. I. D. Hosein, S. H. Lee and C. M. Liddell, *Adv Funct Mater*, 2010, **20**, 3085-3091.
17. F. Ma, S. Wang, L. Smith and N. Wu, *Adv Funct Mater*, 2012, **22**, 4334–4343.

Soft Matter Accepted Manuscript

18. S. Hernández-Navarro, J. Ignés-Mullol, F. Sagués and P. Tierno, *Langmuir*, 2012, **28**, 5981-5986.
19. H. R. Sheu, M. S. Elaasser and J. W. Vanderhoff, *Journal of Polymer Science Part a-Polymer Chemistry*, 1990, **28**, 653-667.
20. H. R. Sheu, M. S. Elaasser and J. W. Vanderhoff, *Journal of Polymer Science Part a-Polymer Chemistry*, 1990, **28**, 629-651.
21. E. B. Mock, H. {De Bruyn}, B. S. Hawkett, R. G. Gilbert and C. F. Zukoski, *Langmuir* 2006, **22**, 4037-4043.
22. J. W. Kim, R. J. Larsen and D. A. Weitz, *J Am Chem Soc*, 2006, **128**, 14374-14377.
23. E. B. Mock and C. F. Zukoski, *Langmuir* 2010, **26**, 13747-13750.
24. J. G. Park, J. D. Forster and E. R. Dufresne, *J Am Chem Soc*, 2010, **132**, 5960-5961.
25. A. V. Delgado, E. Gonzalez-Caballero, R. J. Hunter, L. K. Koopal and J. Lyklema, *Pure and Applied Chemistry*, 2005, **77**, 1753-1805.
26. G. H. Wannier, *Phys Rev*, 1950, **79**, 357-364.
27. Y. Han, Y. Shokef, A. M. Alsayed, P. Yunker, T. C. Lubensky and A. G. Yodh, *Nature*, 2008, **456**, 898-903.
28. Y. Shokef and T. C. Lubensky, *Physical Review Letters*, 2009, **102**, 048303.
29. W. D. Ristenpart, I. A. Aksay and D. A. Saville, *J. Fluid. Mech.*, 2007, **575**, 83-109.
30. D. C. Prieve, P. J. Sides and C. L. Wirth, *Curr. Opin. Colloid. Interface. Sci.*, 2010, **15**, 160-174.
31. H. Zhao, *Electrophoresis*, 2011, **32**, 2232-2244.
32. H. Zhou, M. A. Preston, R. D. Tilton and L. R. White, *J Colloid Interf Sci*, 2005, **285**, 845-856.
33. V. N. Shilov, A. V. Delgado, F. Gonzalez-Caballero and C. Grosse, *Colloid Surface A*, 2001, **192**, 253-265.
34. A. P. Hynninen and M. Dijkstra, *Phys Rev E*, 2005, **72**, 051402.
35. C. S. Dutcher, T. J. Woehl, N. H. Talken and W. D. Ristenpart, *Phys Rev Lett*, 2013, **111**, 128302.
36. T. B. Jones, *Electromechanics of Particles*, Cambridge University Press, 1995.
37. A. T. Chwang and T. Y. Wu, *J. Fluid. Mech.*, 1976, **75**, 677-689.
38. N. Osterman, D. Babič, I. Poberaj, J. Dobnikar and P. Ziherl, *Physical Review Letters*, 2007, **99**, 248301.
39. P. H. Poole, F. Sciortino, U. Essmann and H. E. Stanley, *Nature*, 1992, **360**, 324-328.
40. G. Malescio and G. Pellicane, *Nat Mater*, 2003, **2**, 97-100.
41. W. D. Ristenpart, I. A. Aksay and D. A. Saville, *Phys Rev Lett*, 2003, **90**, 128303.

Soft Matter Accepted Manuscript

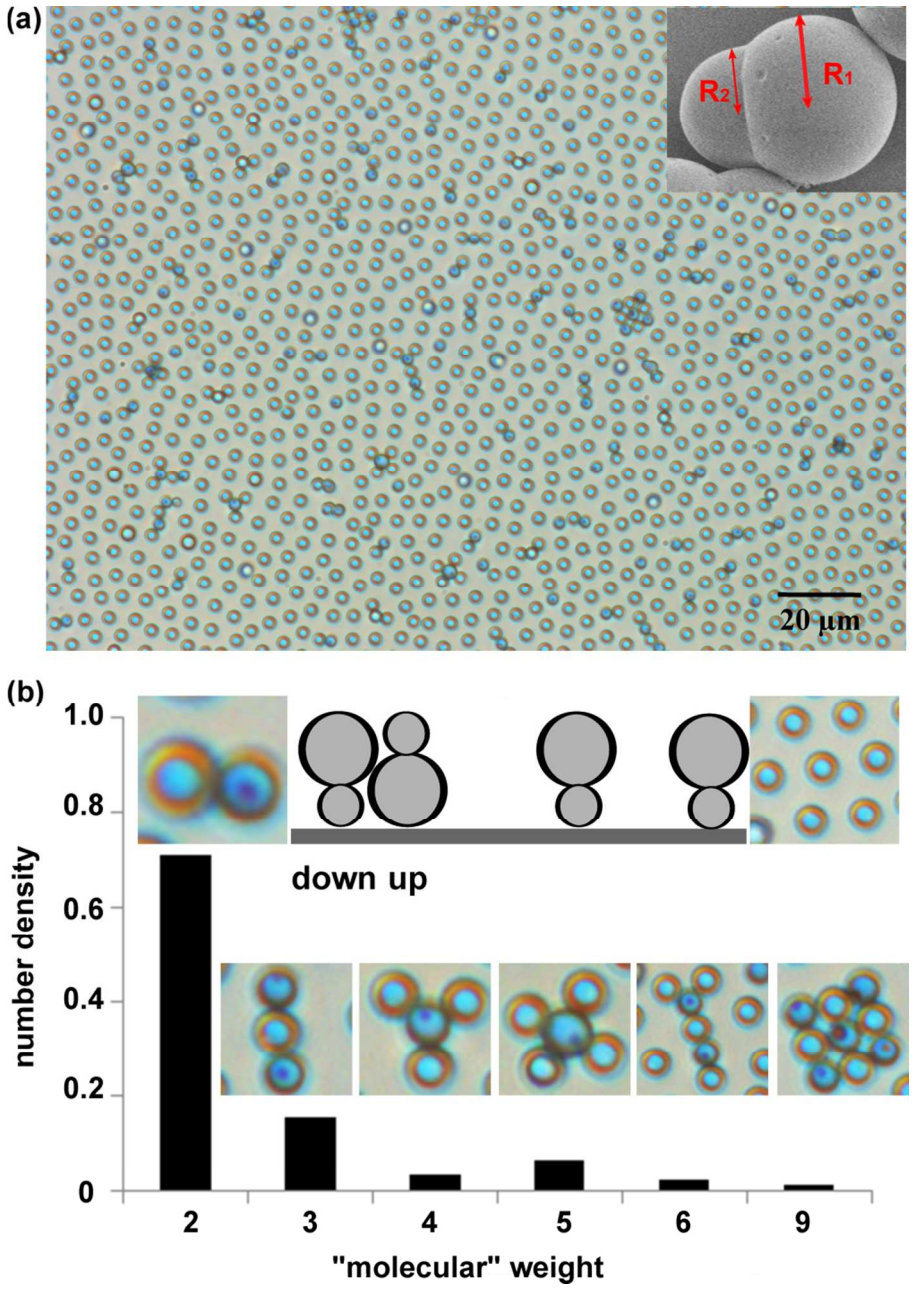

Figure 1 Small clusters formed by oppositely-oriented dimers. (a) Association of standing dimers into colloidal clusters under an AC electric field ($\omega \sim 3$ kHz, $V_p \sim 9$ V). Inset: a SEM image of the asymmetric dimers ($R_1 \sim 1.27$ μm and $R_2 \sim 0.89$ μm). (b) The number fraction of clusters with different "molecular" weights. When focused on the substrate using an inverted microscope, the "down" dimer exhibits a "halo". The "up" dimer exhibits a dark spot due to the stronger scattered light from small dimples of the larger lobe.

Soft Matter Accepted Manuscript

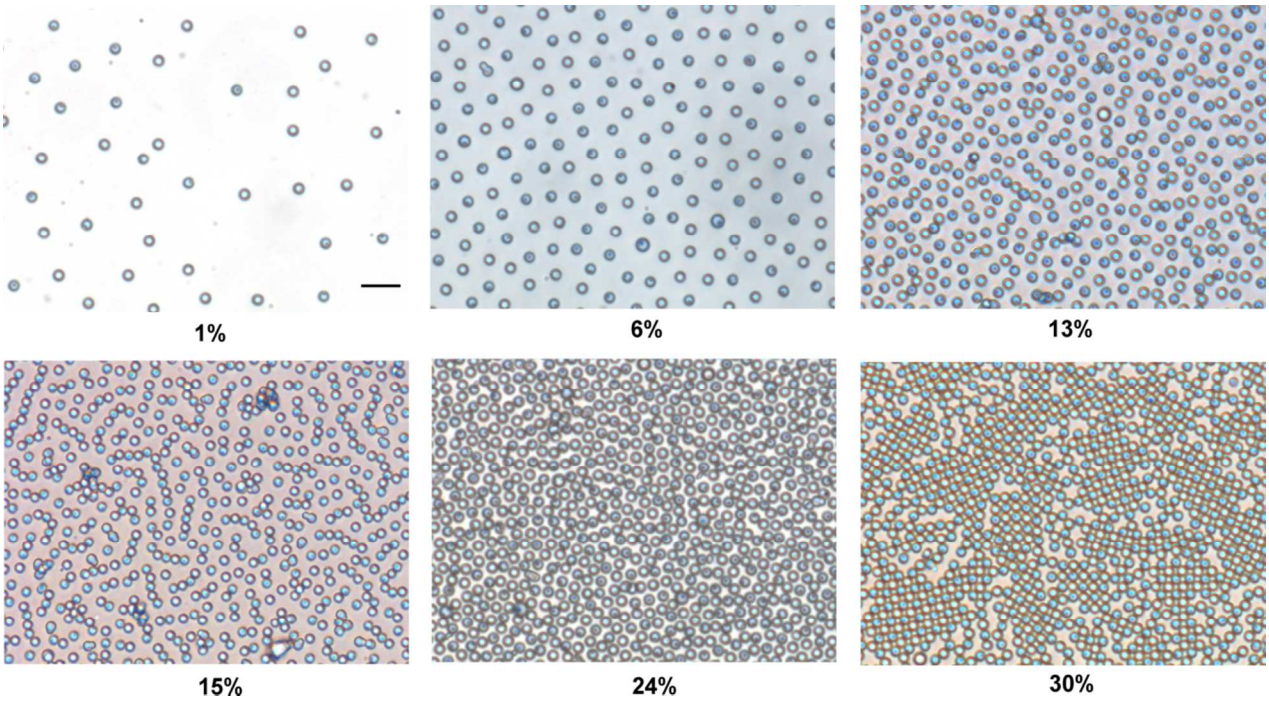

Figure 2 Optical images of the standing dimers at different particle densities ($V_p \sim 10$ V and $\omega \sim 6.5$ kHz). Scale bar for all images: 20 μm.

Soft Matter Accepted Manuscript

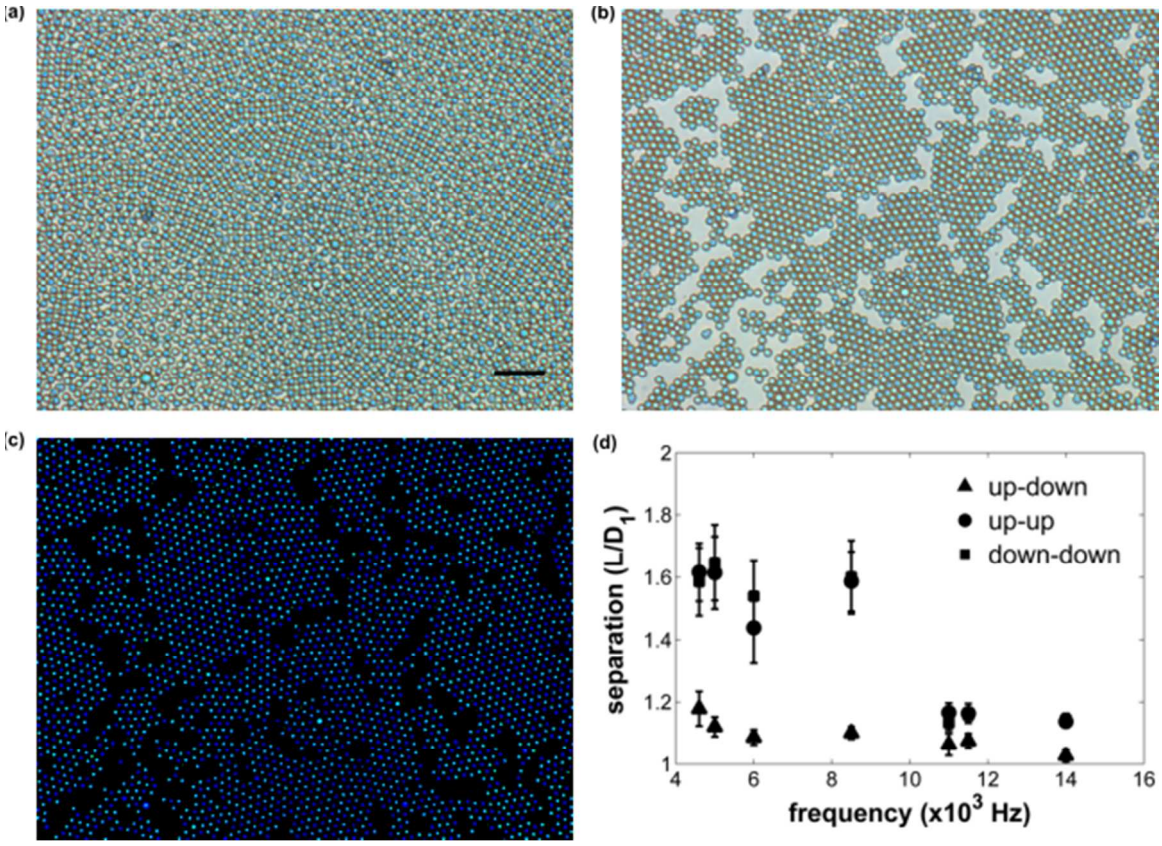

Figure 3 Transformation from square (a) to triangular (b) lattices when the frequency increases from $\omega = 8.5$ kHz to $\omega = 11.5$ kHz. Scale bar for all images: 20μm. (c) Contrast enhancement of (b) reveals the zigzag stripes in the triangular lattice. Dark and bright dots represent the "up" and "down" dimers, respectively. (d) Changes in the dimer-dimer separation in the square and triangular lattices with an increasing frequency.

Soft Matter Accepted Manuscript

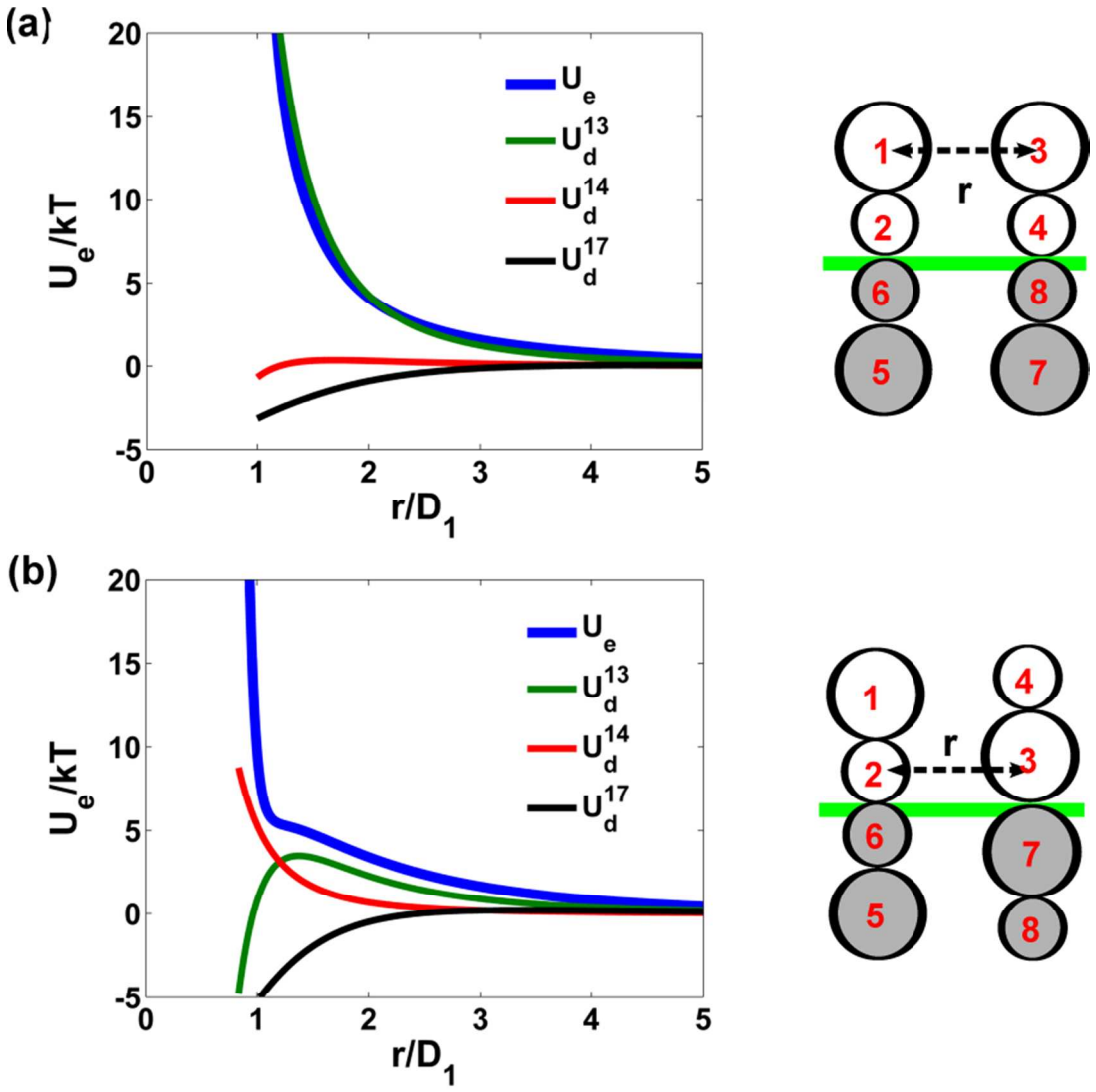

Figure 4 The electrostatic (screened Coulomb and dipolar) interaction U_e between dimers. (a) U_e (scaled by the thermal energy) between "down" dimers and breakdown of the contribution from dipolar interactions U_d^{ij} between different lobes. The system of dimers is approximated by individual spheres. The substrate is illustrated in green and grey spheres are (charge and dipole) images. The separation is scaled by the large lobe diameter D_1. (b) U_e and U_d^{ij} for a pair of "down" and "up" dimers.

Soft Matter Accepted Manuscript

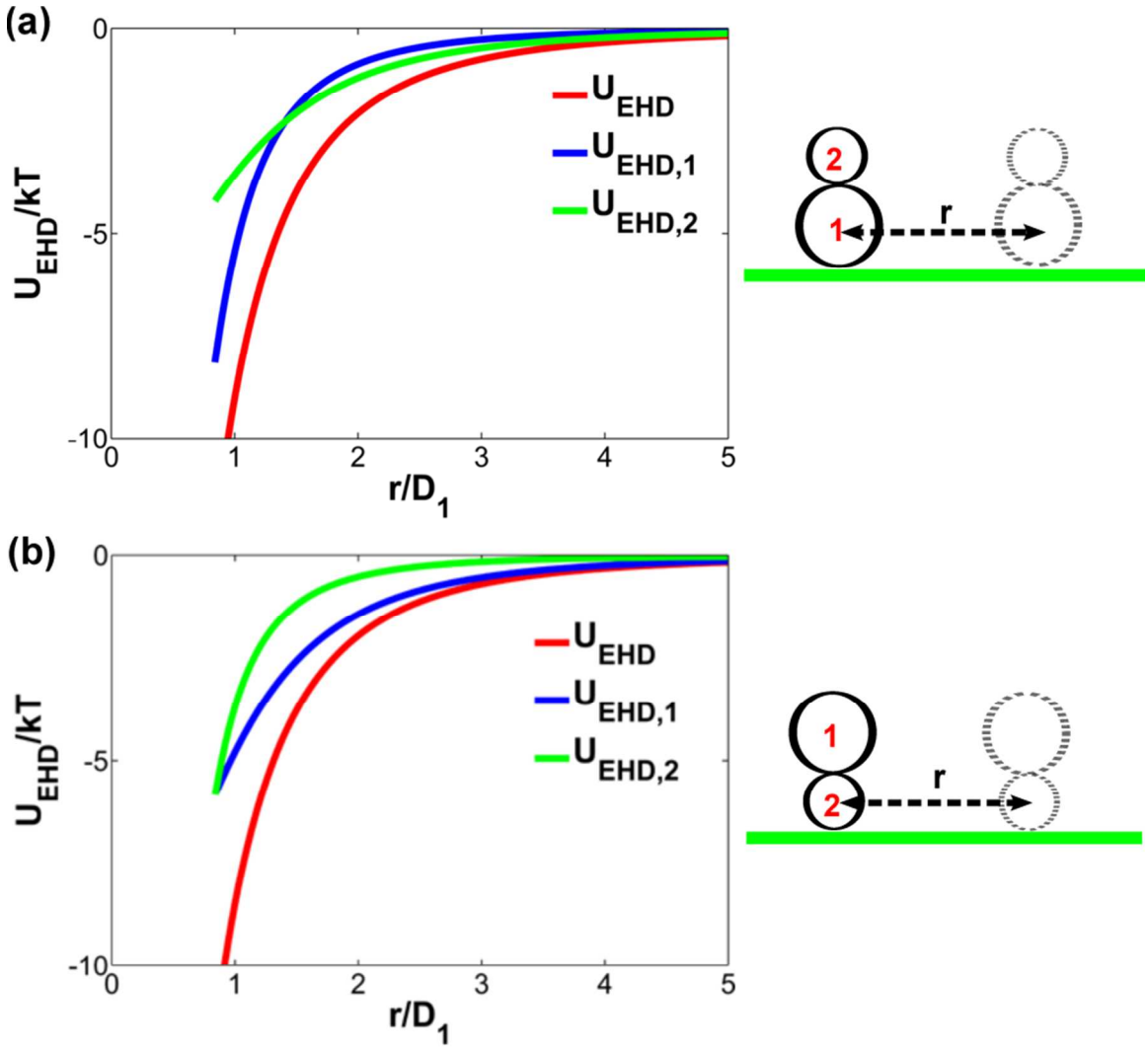

Figure 5 The electrohydrodynamic (EHD) interaction between dimers. (a) U_{EHD} (scaled by the thermal energy) between a pair of "up" dimers and the contributions from each lobe $U_{EHD,i}$. (b) U_{EHD} and $U_{EHD,i}$ for two "down" dimers. The separation is scaled by the large lobe diameter D_1.

Soft Matter Accepted Manuscript

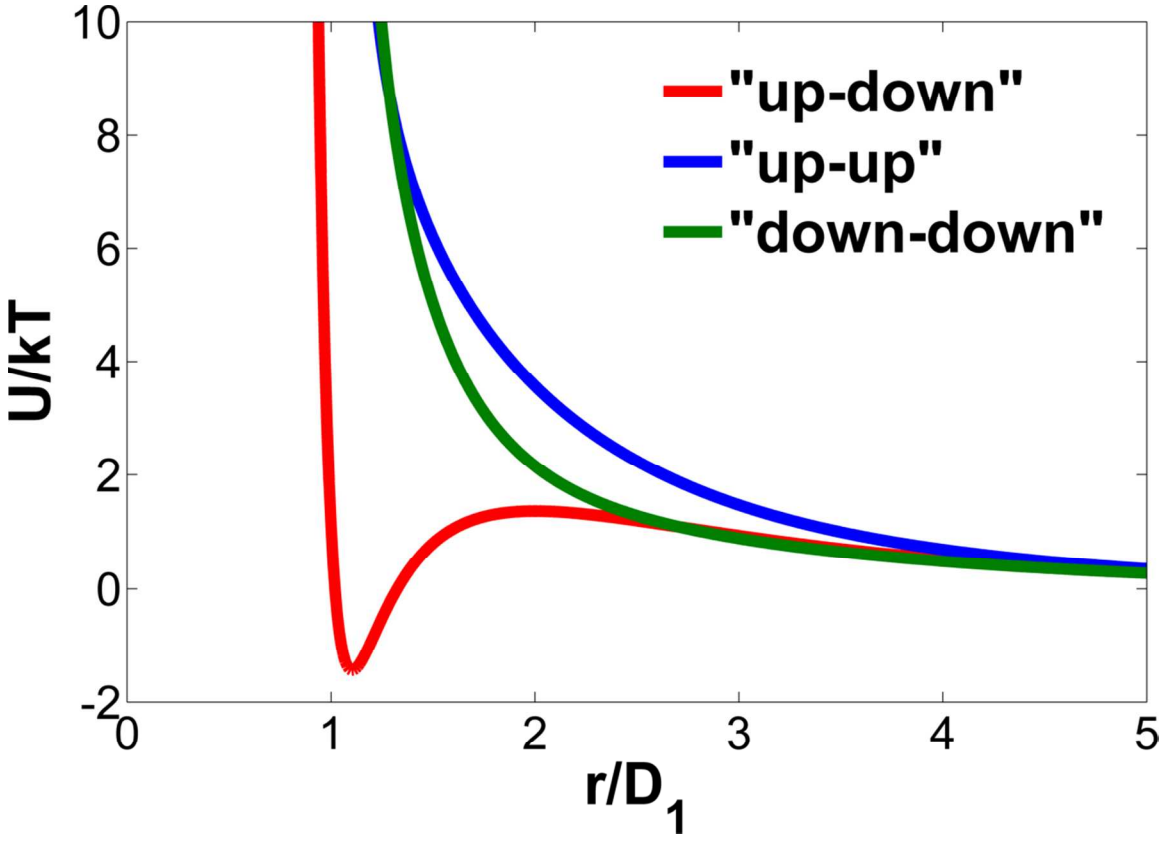

Figure 6 The overall (electrostatic and electrohydrodynamic) interaction between a pair of asymmetric dimers with different orientations.

Soft Matter Accepted Manuscript

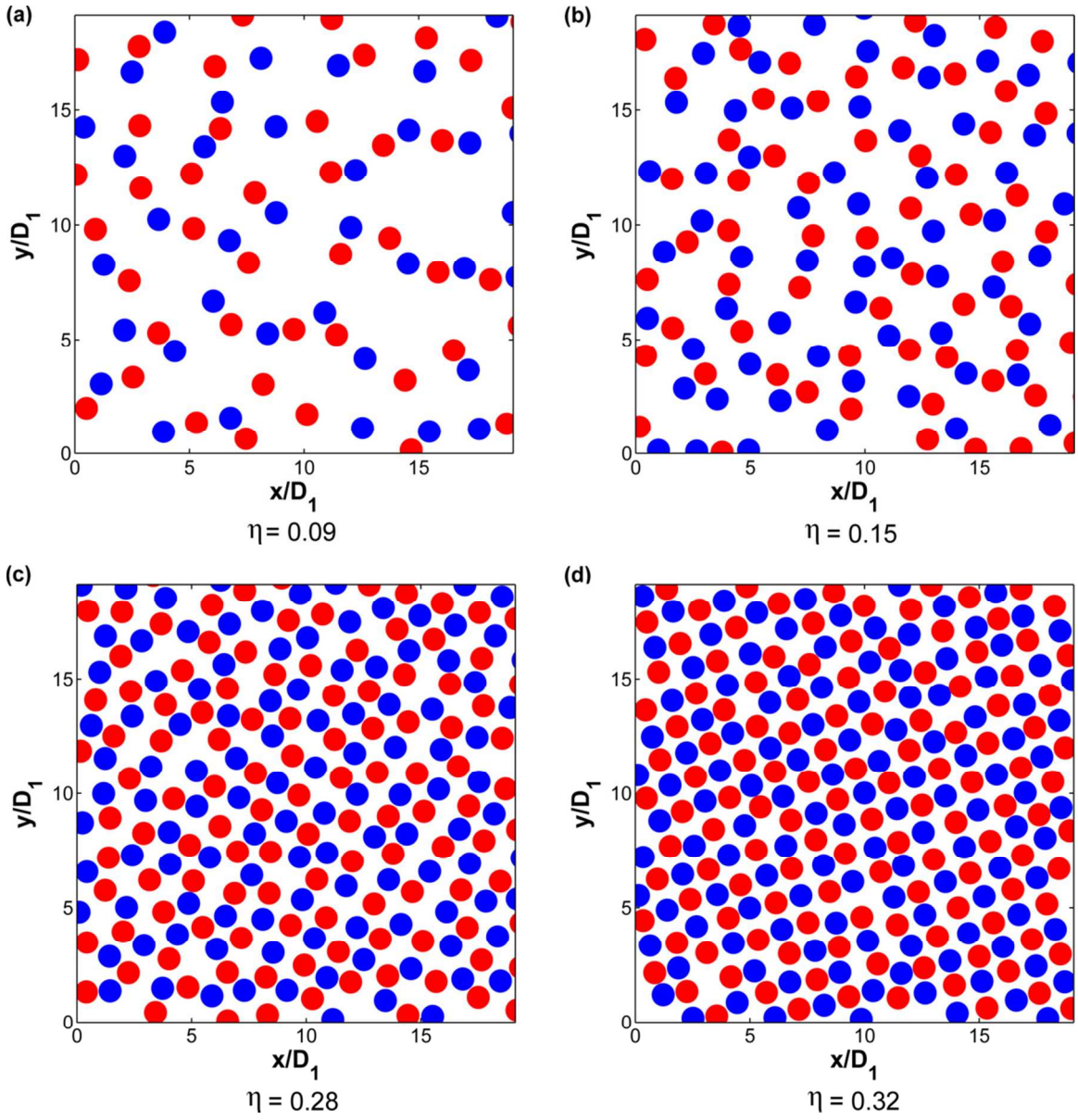

Figure 7 Top-view snap shots from Monte Carlo simulation (*NAT*) of $N_{tot} = 256$ dimers at different particle densities. Blue and red discs represent "up" and "down" dimers, respectively. The simulation parameters are consistent with the experimental conditions in Fig. 2.

Soft Matter Accepted Manuscript

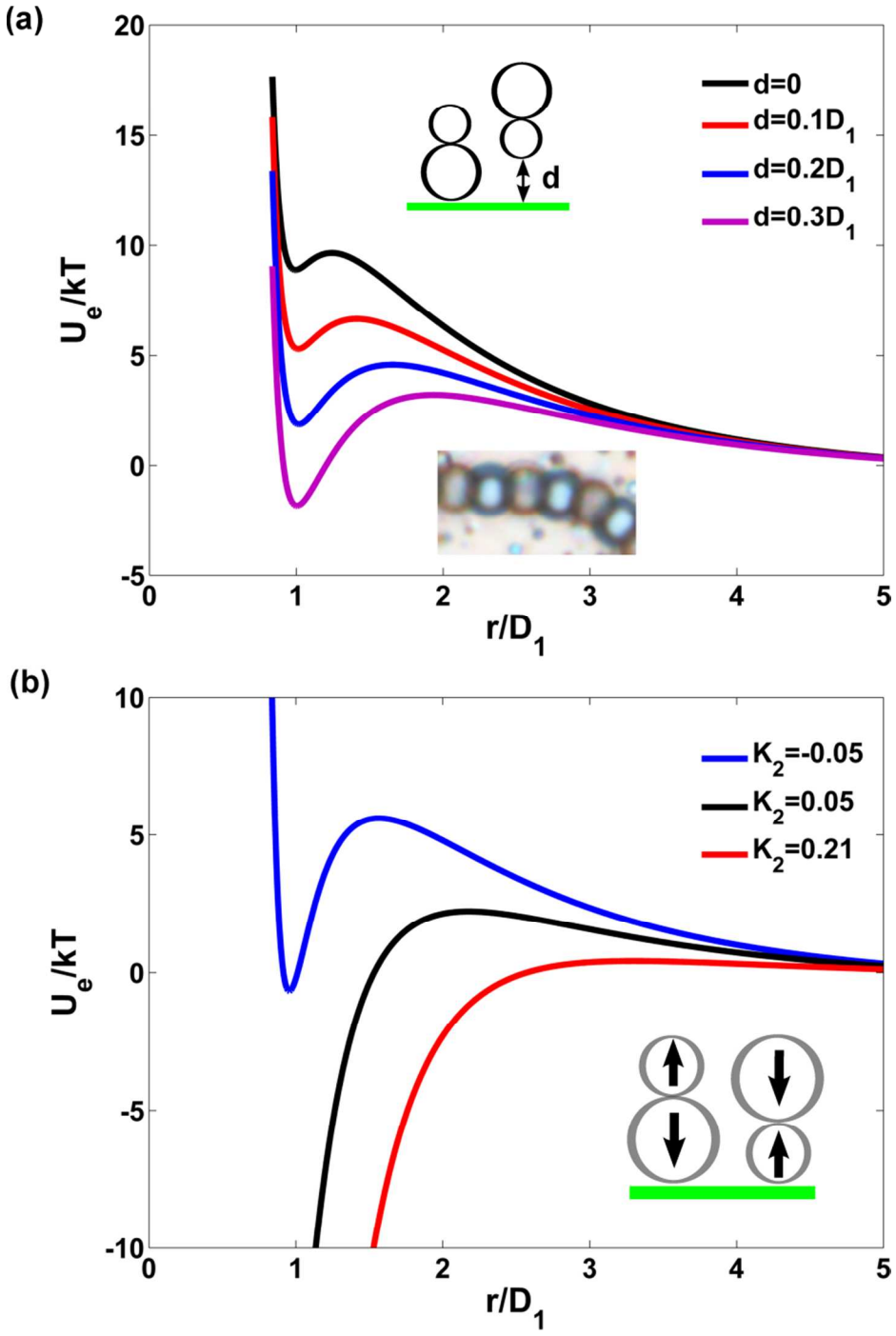

Figure 8 The impacts of particle lifting and polarizabilities on pair interaction. (a) The "up-down" electrostatic interaction when one dimer is lifted above the substrate. (b) The "up-down" electrostatic interaction when the dimer has anisotropy in polarization coefficients. K_1 is fixed (~-0.21) for all three curves. The arrows in the inset illustrate the directions of induced dipoles when $K_2 > 0$.

Soft Matter Accepted Manuscript

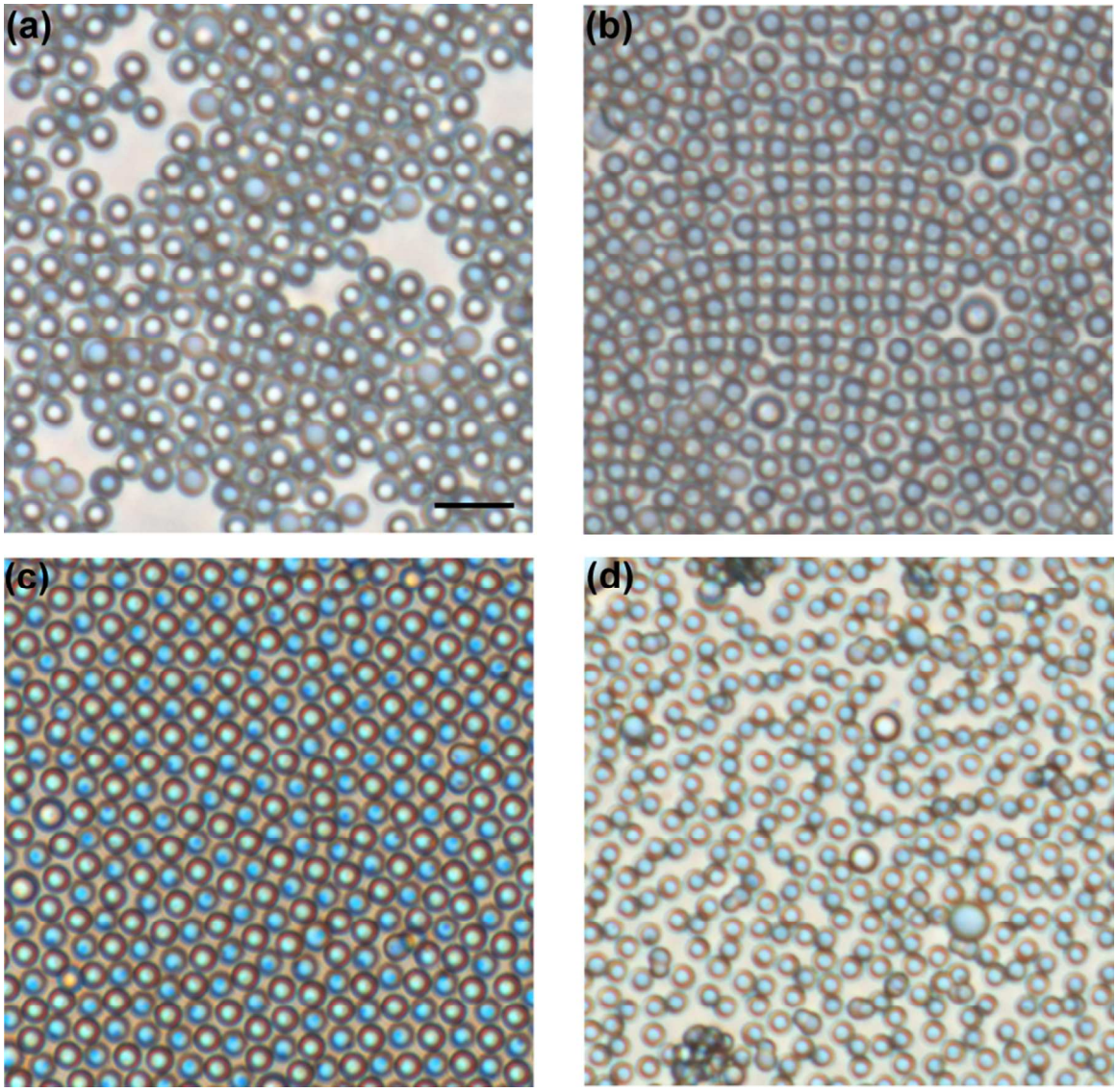

Figure 9 Alternating association between "up" and "down" dimers with different aspect ratios. (a) $R_2 / R_1 = 0.57$; (b) $R_2 / R_1 = 0.67$; (c) $R_2 / R_1 = 0.7$; and (d) $R_2 / R_1 = 0.86$. Scale bar for all images: 10 μm. The optical contrast for (d) has been adjusted to distinguish the "up" and "down" dimers.

Soft Matter Accepted Manuscript

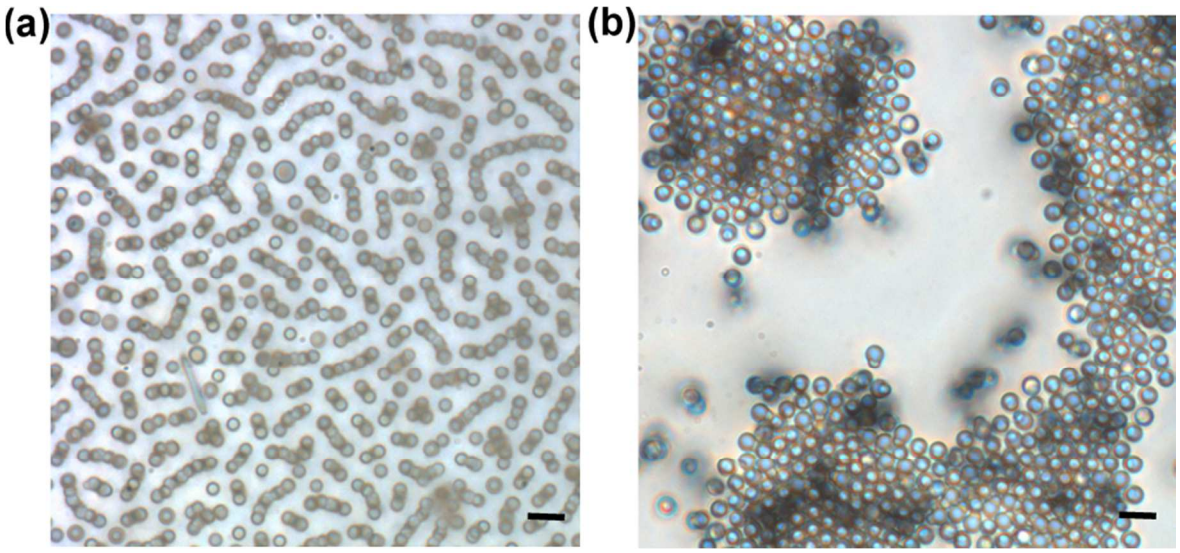

Figure 10 Pattern formation when the electrostatic and electrohydrodynamic interactions are not balanced. (a) The zig-zag clusters and linear chains of standing dimers in DMSO due to the stronger out-of-plane dipolar attraction between neighboring dimers ($V_p = 8$ V and $\omega = 2.2$ kHz). (b) The hexagonal array of standing dimers in 1mM KCl aqueous solution where the electrohydrodynamic interaction dominants ($V_p = 7$ V and $\omega = 4.2$ kHz). Scale bars: 10 μm.

Soft Matter Accepted Manuscript

Table of Contents

The orientation-dependent interactions between asymmetric dimers induce a series of colloidal structures that closely resemble one- and two-dimensional antiferromagnetic lattices under AC electric fields.

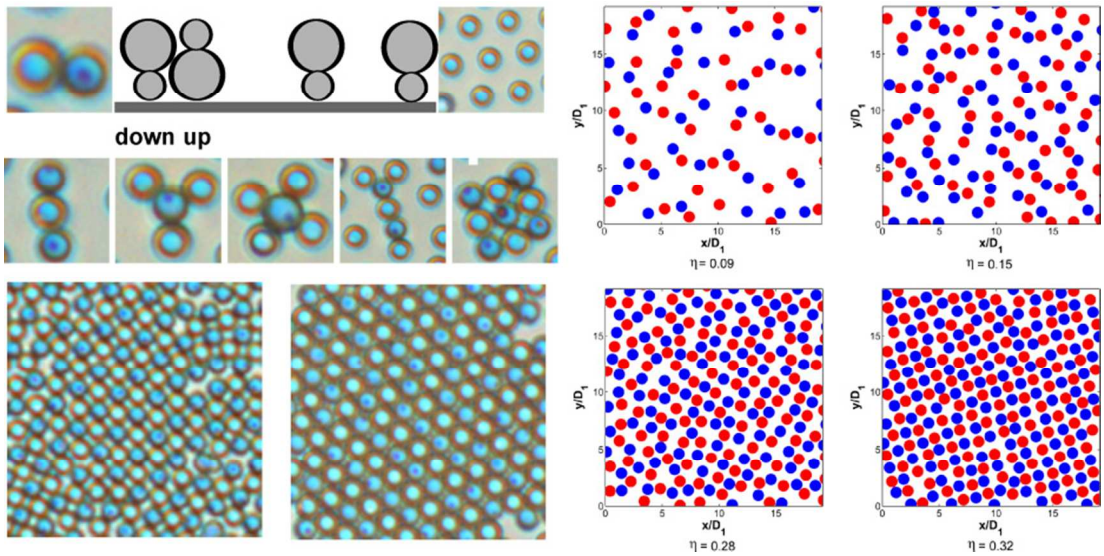

Soft Matter Accepted Manuscript

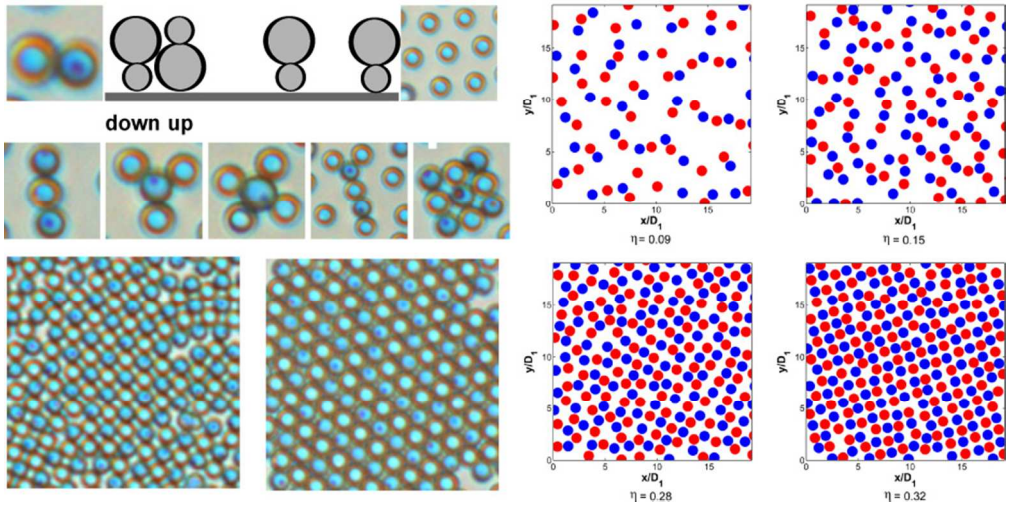

The orientation-dependent interactions between asymmetric dimers induce a series of colloidal structures that closely resemble one- and two-dimensional antiferromagnetic lattices under AC electric fields.
78x39mm (300 x 300 DPI)

Soft Matter Accepted Manuscript